



## OPEN Fecal transplantation from humans with obesity to mice drives a selective microbial signature without impacting behavioral and metabolic health

Audrey M. Neyrinck<sup>1,9</sup>, Hany Ahmed<sup>2,9</sup>, Quentin Leyrolle<sup>1,3,9</sup>, Sophie Leclercq<sup>4</sup>, Camille Amadieu<sup>1,3</sup>, Topi Meuronen<sup>2</sup>, Sophie Layé<sup>3</sup>, Patrice D. Cani<sup>1,5,6</sup>, Olli Kärkkäinen<sup>7,8</sup>, Laure B. Bindels<sup>1,5</sup>, Kati Hanhineva<sup>2,10</sup> & Nathalie M. Delzenne<sup>1,10</sup>✉

Obesity is associated with alterations in the gut microbiome that may contribute to metabolic and mental health disturbances. Fecal microbiota transplantation (FMT) from humans to mice is a model proposed to study human microbiota-associated disorders. In this study, we investigated whether gut microbiota from human donors with obesity could affect behavior and metabolomic profiles of mice. Stools from donors with obesity and from lean donors were inoculated to antibiotic-pretreated mice fed a standard low-fat diet throughout the experiment. Obese-recipient mice exhibited a lower bacterial alpha-diversity and limited changes in specific taxa (e.g., an increase in *Eubacterium*) but were similar to lean-recipient mice in terms of dietary intake, body weight, fat mass, anxiety/depression-like behavior and glucose homeostasis. Non-targeted LC–MS metabolomic analysis revealed no change in the portal and cava serum samples. However, 1-methylnicotinamide, indole-3-acetic acid (I3A) and methyllysine were increased in the cecal content of obese-recipient compared to lean-recipient mice. Microbial metabolites derived from amino acids were positively correlated with *Eubacterium*. These results indicate that FMT from donors with obesity to mice fed chow diet (low in lipids) leads to minor but persistent change in intestinal microbial-derived metabolites, without recapitulating the metabolic and behavioral alterations of obesity.

The etiological triad of diet, genome, and gut microbiota plays a crucial role in the pathophysiology of obesity, considered a pandemic of the 21st century. The exploration of the role of the microbiome in obesity and metabolic diseases has been supported by experiments of fecal microbiome transfer (FMT). Studies conducted in diabetic patients have shown that heterologous FMT from non-diabetic to diabetic subjects can improve insulin sensitivity. However, the effectiveness of this treatment is temporary and varies between individuals<sup>1,2</sup>. FMT from human donors to recipient mice has also been performed to investigate the causal role of the gut microbiota on physiology and its impact on responses to nutritional disorders. Notably, humanized mice fed the Western diet exhibit increased adiposity, a trait that can be transmitted through microbiota transplantation<sup>3</sup>. We have previously demonstrated that the improvement of metabolic alterations by a dietary fiber (inulin) in mice transplanted with the gut microbiome from patients with obesity was variable. This variability depended on both the microbiome characteristics of the donor and changes in specific bacterial taxa following inulin feeding<sup>4</sup>.

<sup>1</sup>Metabolism and Nutrition Research Group, Louvain Drug Research Institute (LDRI), UCLouvain, Université catholique de Louvain, Brussels, Belgium. <sup>2</sup>Food Sciences Unit, Department of Life Technologies, University of Turku, Turku, Finland. <sup>3</sup>INRAE, Bordeaux INP, NutriNeuro, UMR 1286, Université de Bordeaux, 33000 Bordeaux, France. <sup>4</sup>Laboratory of Nutritional Psychiatry, Institute of Neuroscience, UCLouvain, Université catholique de Louvain, Brussels, Belgium. <sup>5</sup>WELBIO Department, WEL Research Institute, Wavre, Belgium. <sup>6</sup>Institute of Experimental and Clinical Research (IREC), UCLouvain, Université catholique de Louvain, Brussels, Belgium. <sup>7</sup>School of Pharmacy, University of Eastern Finland, Kuopio, Finland. <sup>8</sup> Institute of Public Health and Clinical Nutrition, University of Eastern Finland, Kuopio, Finland. <sup>9</sup>Audrey M. Neyrinck, Hany Ahmed and Quentin Leyrolle contributed equally to this work. <sup>10</sup>These authors jointly supervised the work: Kati Hanhineva and Nathalie M. Delzenne. ✉email: Nathalie.Delzenne@uclouvain.be

Obesity is often accompanied by alterations in psychological traits, which can lead to depression, altered social behavior or addictions<sup>5</sup>. The gut-brain axis plays as crucial in human mental health and behavior, with the gut microbiome being a key component of this axis. This is primarily due to its production of neurotransmitters or other bioactive metabolites involved in neuroendocrine processes<sup>6–8</sup>.

Metabolomics, i.e. the systematic identification and quantitation of all compounds involved in metabolic pathways (metabolites) within a given organism or biological sample<sup>9</sup>, is a valuable method for elucidating the crosstalk between host metabolism and gut microbiota<sup>8,10</sup>. Numerous studies have shown that the serum metabolome contains a plethora of biomarkers and causative agents of various diseases. Some of these metabolites have been taken up from the environment while others are produced endogenously. The origins of specific metabolites are known, including those that are highly heritable, as well as those influenced by lifestyle choices (e.g. smoking), diet or the gut microbiome. Analysis of the fecal gut microbiota and plasma non-targeted metabolomics in subjects with increased negative mood revealed elevated levels of *Coprococcus* and decreased levels of *Sutterella* and *Lactobacillus*<sup>11</sup>. Serum metabolomic analysis in these subjects showed altered levels of several amino acid-derived metabolites, including an increase in L-histidine and a decrease in phenylacetylglutamine. These changes are associated with altered gut microbiota composition and function rather than differences in dietary amino acid intake<sup>11</sup>. However, the proof of concept that the gut microbiome characteristics drive the occurrence of psychological trait has not yet been fully demonstrated.

In a previous study, we demonstrated that transplanting the gut microbiota from patients with alcohol-use disorder into mice replicated some behavioral changes linked to alcohol dependence, including reduced sociability, increased depression-like behavior, and higher stress level. We also showed that FMT lead to changes in the production of bacterial-derived metabolites (namely ethanol) which may explain the brain-dysfunction associated with the altered microbiome<sup>12</sup>. Here, we hypothesized that the gut microbiome associated with obesity in humans might drive behavioral changes independent of effects on adiposity or metabolic disorders. The objective of this study was to determine whether FMT from human donors with obesity—who exhibit varying levels of psychological mood scores—can trigger changes in the production of metabolites related to metabolic and behavioral traits (sociability, depression) in recipient mice. To investigate this, we conducted untargeted metabolomics analyses of the serum and intestinal contents of the recipient mice to explore the potential contribution of gut microbiome, nutrition- or host-derived metabolites.

## Results

### Experimental design

Ten donors with obesity (7 men and 3 women) and 5 lean control donors (3 men and 2 women) were selected based on their body mass index (BMI) in order to inoculate fecal microbiota into recipient antibiotic pretreated-mice (Table S1). Although the psychological mood score, assessed using the Positive and Negative Affect Schedule (PANAS), were slightly lower in individuals with obesity, the difference was not significant ( $p = 0.09$ ). Forty mice receiving “obese” microbiota (obese-recipient mice) and 20 mice that receive a “lean” microbiota (lean-recipient mice) were fed a normal chow diet for the duration of the experiment. They also underwent behavioral tests and oral glucose tolerance test according to the experimental design outlined in Fig. 1 (4 recipient mice/donor; 2 independent experiments). Based on the Aitchison distance-based hierarchical clustering of the microbiome of donors and recipient mice (Fig. S1), we decided to exclude 1 donor and 6 mice from the statistical analyse for all the parameters discussed in the next sections.

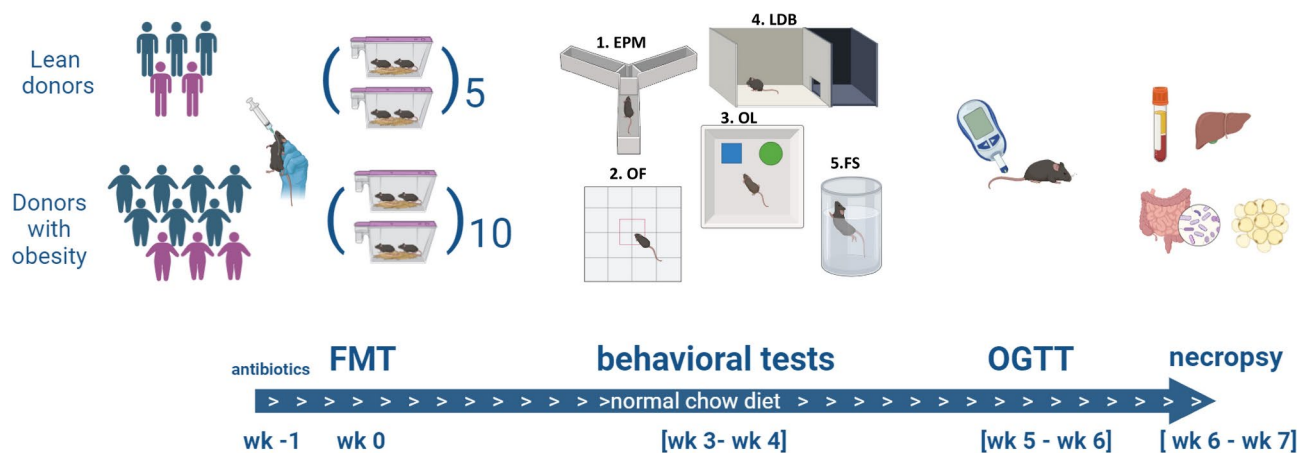


**Fig. 1.** Experimental design of mice study. Fecal microbiota transfer (FMT) from donors with obesity (7 men, 3 women) or lean donors (3 men, 2 women) into antibiotic-pretreated male mice. Mice were fed a normal chow diet for 6–7 to weeks following the FMT. Behavioral tests (1. elevated plus maze (EPM); 2. open field (OF); 3. object location (OL); 4. light and dark box (LDB); 5. forced swim (FS)) were performed 3–4 weeks after FMT. Oral glucose tolerance test (OGTT) were assessed 5–6 weeks after FMT. Created in BioRender. Neyrinck, A. (2025) <https://BioRender.com/j25w456>.

## Characterization of the caecal microbiota of the recipient mice

The number of total bacteria per gram of caecal matter of recipient mice was similar to the number of total bacteria per gram of fecal matter of human donors Fig. S1. Finally, 48% and 53% of genera present in the control and obese inocula (the percentages were determined from the number of genera found in the caecal content of recipient mice relative to the number of genera detected in the inoculum) were successfully transferred to the respective recipient mice.

Compared with the microbiota from lean-recipient mice, the microbiota of obese-recipient mice exhibited a reduced bacterial  $\alpha$ -diversity (Shannon index, Fig. S2) and a modest change in  $\beta$ -diversity (only at the genus level, evidenced from the PERMANOVA analyses) (Fig. 2a). *Eubacterium* was the main genus explaining the shift alongside the first component of the PCA of the obese-recipient mice compared to the lean-recipient mice (Fig. 2a). *Eubacteriaceae* is the sole family significantly increased in obese-recipient versus lean-recipient mice (Supplementary Dataset 1). Consistently, at the genus level, *Eubacterium* was more abundant in the caecum of obese-recipient than in lean-recipient mice (Fig. 2b, Supplementary Dataset 1). Another genus, *Eisenbergiella*, also increased following the transfer of an obese microbiota. Conversely, two genera, *Flavonifractor* and *Barnesiella*, significantly decreased in the caecal content of obese-recipient compared to lean-recipient mice (Fig. 2b, Supplementary Dataset 1).

## Mice inoculated with the obese microbiota exhibit no change regarding behavior and metabolic and inflammatory markers

Body weight evolution and glucose homeostasis, assessed by measuring glycemia and insulinemia at fasting state and after a load of glucose (OGTT), were not affected by the transfer of humanized microbiota from individuals with obesity versus lean-recipient mice (Fig. S3). In addition, there were no significant differences between the groups in circulating levels of corticosterone, leptin, brain-derived neurotrophic factor (BDNF) or several inflammatory parameters (Table S2). To assess the impact of gut microbiota on anxiety/depression-like behavior and memory, recipient mice underwent 6 different tests 3 or 4 weeks after FMT. The light/dark box test, open field test, object location test, elevated-plus maze test and the forced swim test showed no differences in memory and anxiety/depression-like behavior between obese-recipient and lean-recipient mice (Fig. 3).

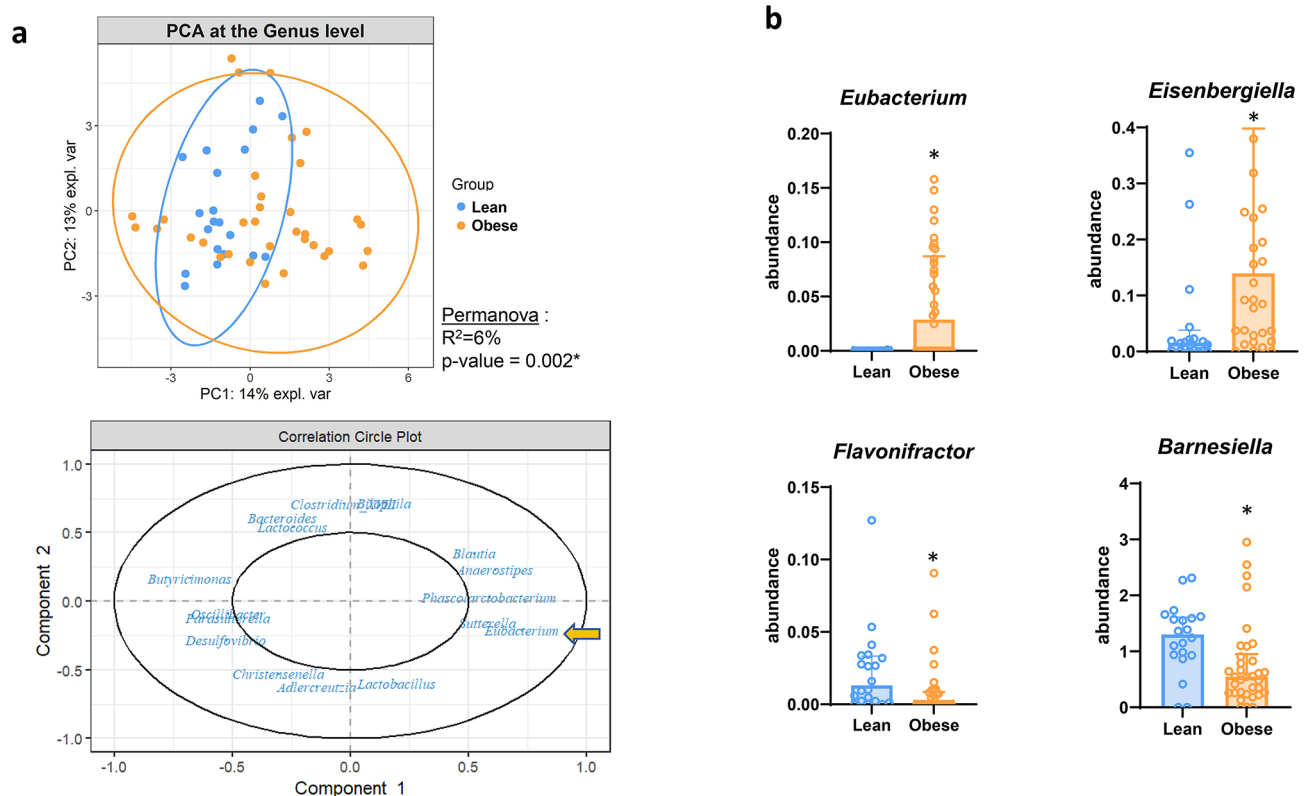


**Fig. 2.** Impact of the transfer of obese and lean human fecal microbiota on mouse caecal microbiota. Antibiotic-pretreated recipient mice were inoculated with microbiota from donors with obesity or from lean donors. PCA plot of all genera based on the Aitchinson distance, with PERMANOVA analysis and correlation circle plot (a). Caecal genera significantly (Data are means  $\pm$  SD; \* $q < 0.05$ , Mann Whitney) altered by obese microbiota transfer (b).

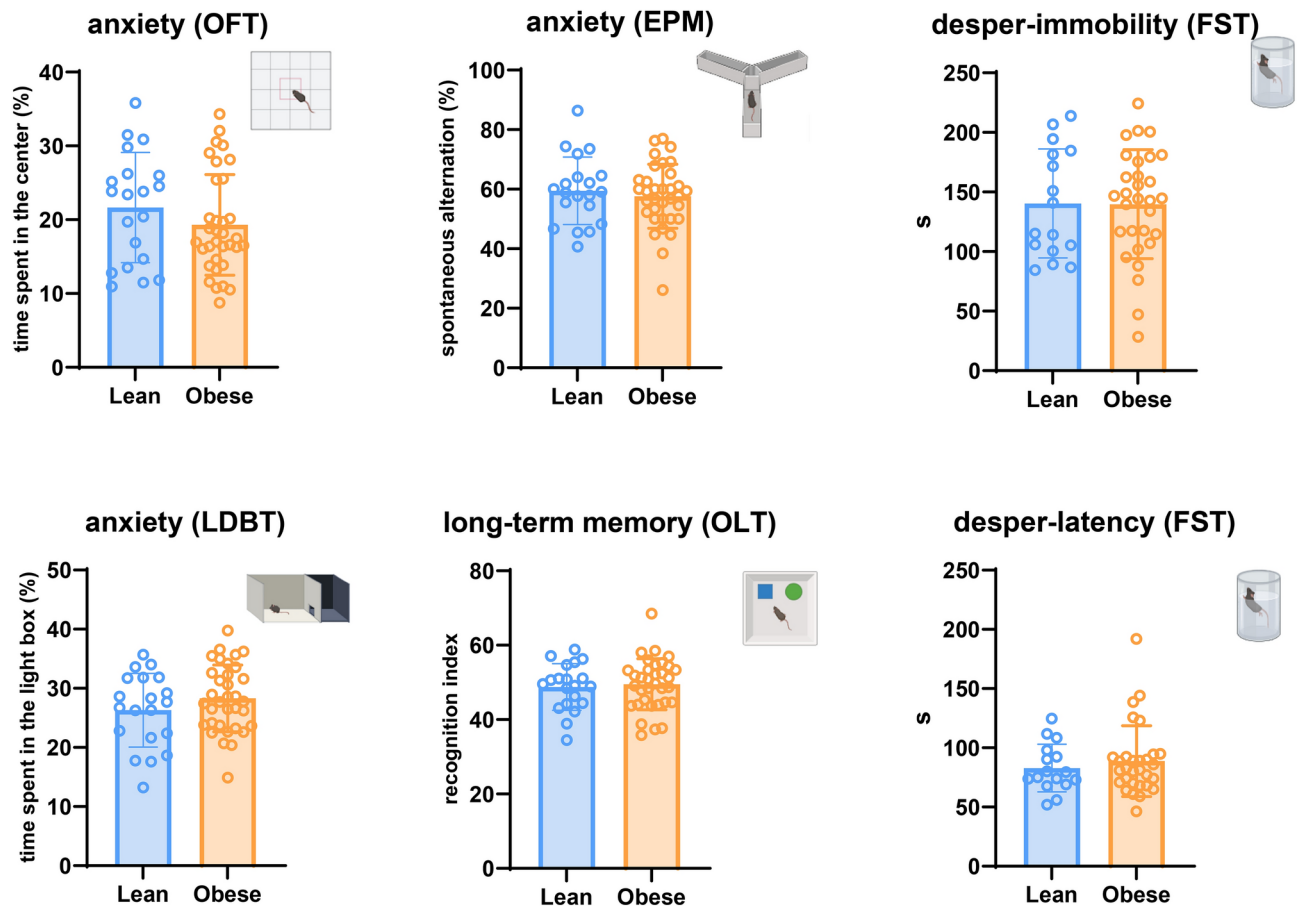


**Fig. 3.** Impact of obese microbiota transfer to mice on anxiety- and depression-like behavior. Antibiotic-pretreated recipient mice were inoculated with microbiota from donors with obesity or from lean donors. Behavioral tests were performed 3–4 weeks after FMT. Data are mean  $\pm$  SD.  $p > 0.05$  (student t test or Mann Whitney). *OFT* open field test, *EPM* elevated plus maze test, *FST* forced swim test, *OLT* object location test, *LDBT* light and dark box test. Parts of the image come from Fig. 1.

### Inoculation with the obese microbiota modulates the metabolome of recipient mice, mainly in the caecum

Metabolomic profiles were analyzed in the caecal content and in the blood from portal vein or vena cava of recipient mice. The complete set of statistical analysis of data is presented in Supplementary Dataset 2. As shown in Fig. 4a, we observed that metabolomic fingerprints were more separated in the caecal content than in blood. Among annotated metabolites that discriminated (i.e. VIP > 2) obese from control recipient mice in the caecal content (Fig. 4b), 3-indoleacetic acid (I3A), 1-methylnicotinamide and N(6)-methyllysine are those that significantly (at the q value < 0.05) increased in obese-recipient versus lean-recipient mice (Fig. 5). Although no metabolite was significantly different in the blood after adjusting for false discovery rate (portal and systemic) between both groups, I3A is one of the metabolites that also increased in the portal blood (+ 57%,  $p = 0.07$ , VIP score = 1.74) and the vena cava blood (+ 36%,  $p = 0.07$ , VIP score = 1.27), in contrast to 1-methylnicotinamide and N(6)-methyllysine that were not significantly modified in the portal or systemic serum (Fig. 4b, Supplementary Dataset 2).

### Increase of 3-indole acetic acid occurring due to inoculation with the obese microbiota is associated to specific bacterial changes

We conducted a correlation analysis between metabolites and bacteria significantly impacted by the inoculation with obese microbiota (Fig. 6a). Interestingly, the *Eubacteriaceae* family, and coherently *Eubacterium*, was identified as a key contributor to the elevated levels of I3A -and to a lesser extent N(6)-methyllysine—in the caecal content of obese-recipient mice. However, no significant correlation was found between the three highlighted caecal metabolites and the behavioral parameters (Fig. 6b). Of note, I3A in the plasma from vena cava was negatively and significantly correlated with anxiety parameter obtained from EPM test (Spearman rank correlation  $r = -0.295$ ,  $p = 0.035$ ).

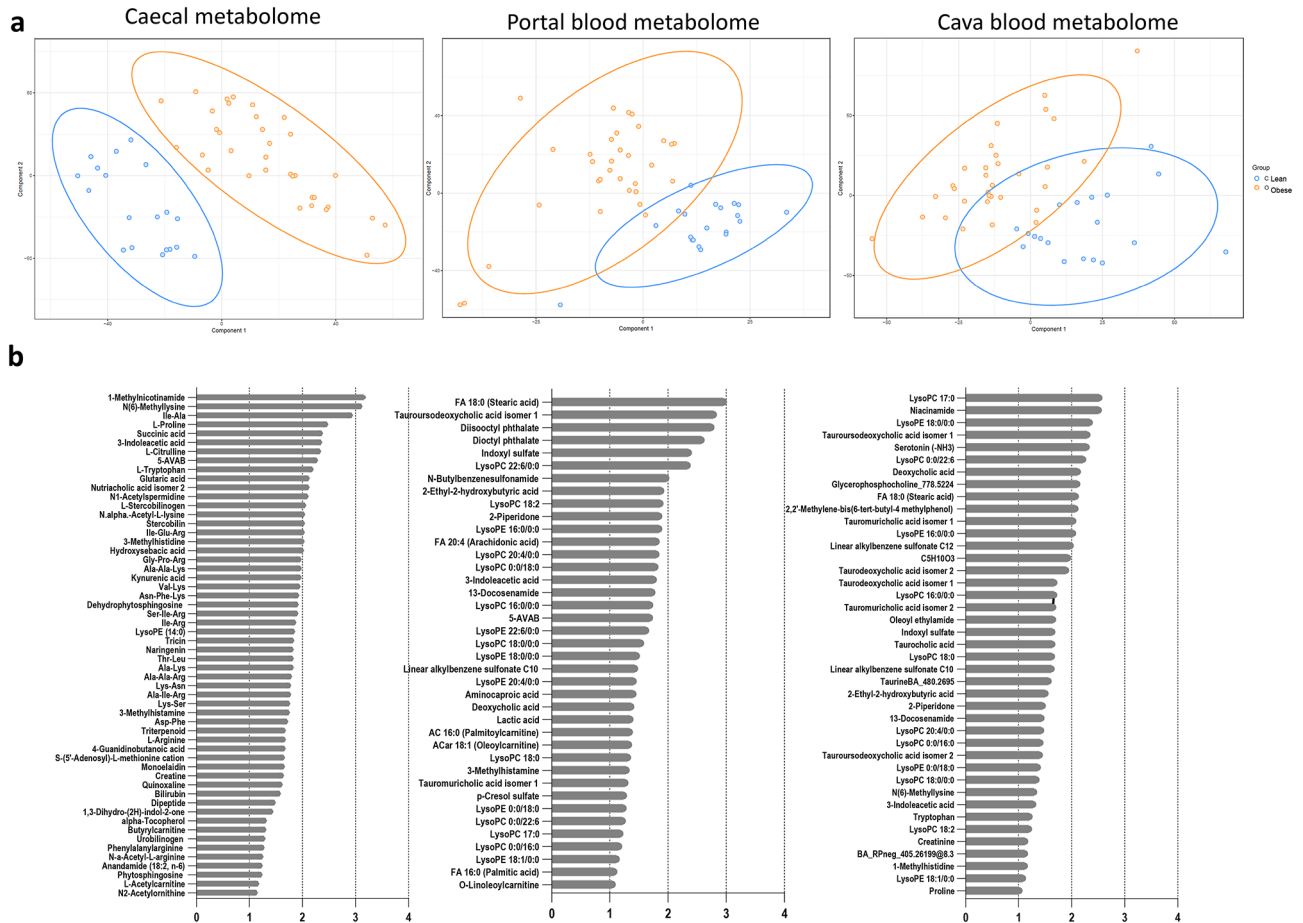


**Fig. 4.** Obese microbiota transfer to mice shapes the caecal and blood metabolome. Antibiotic-pretreated recipient mice were inoculated with microbiota from donors with obesity or from lean donors. Scores plot of the sparse partial least square discriminant analysis (sPLS-DA) of the metabolomic features between obese recipient mice and lean recipient mice (a). Variable importance in projection (VIP) plots with the top discriminating metabolites (VIP score > 1) identified through PLS-DA analyses in descending order of importance (b).

## Discussion

Several studies suggest that the microbiome in obese individuals has an increased capacity to harvest energy from the diet and that this trait is transmissible identifying the gut microbiota as a key contributing factor to the pathophysiology of obesity<sup>13</sup>. For instance, microbiota transplantation from mice previously fed an obesogenic diet to lean germ-free recipients results in a greater increase in fat mass compared to transplants from lean donors. Furthermore, FMT from leptin-deficient *ob/ob* mice to germ free mice leads to a significantly greater increase in total body fat than FMT from lean littermates *ob/+* or *+/+* mice<sup>14</sup>. However, our data indicated that when mice are fed a chow diet (low in fat) after FMT from a human obese donor compared to a lean donor, there is no difference in fat mass, glycemia, or markers of inflammation. This finding contradicts previous observations of an obese phenotype transfer from obese human donor to germ-free mice: germ-free mice colonized with fecal microbiota from each member of four twin pairs discordant for obesity conveyed significantly greater increases in body mass and adiposity than those of lean communities<sup>4</sup>. The lack of effect on body weight, adiposity and glucose homeostasis due to FMT from obese human donors has already been described by Rodriguez et al.<sup>15</sup>. They showed that mice inoculated with fecal matter from obese human donors (after microbiome depletion with antibiotics) had a significantly different microbiome compared to mice that received a FMT from lean donors. Interestingly, Rodriguez et al. highlighted that diet influenced the microbiome composition irrespective of donor body type after 22 weeks of treatment, suggesting that diet is a key variable in the shaping of the gut microbiome after FMT. It is important to note that in the present study, we deliberately chose to provide a chow diet low in lipid to the mice to avoid any interference from nutrients and fat components on inflammation.

The data presented in this paper refute the initial hypothesis that transferring the gut microbiome from patients with obesity modifies anxiety/depressive behavior in mice. Even if there is no change in metabolism and behavior in mice transferred with the gut microbiome from donors with obese versus lean phenotype, it is quite interesting to note that some specific modifications of selected bacteria, and of bacterial-related metabolites are present up to 7 weeks after the transplantation process. The question of the relevance of those microbial

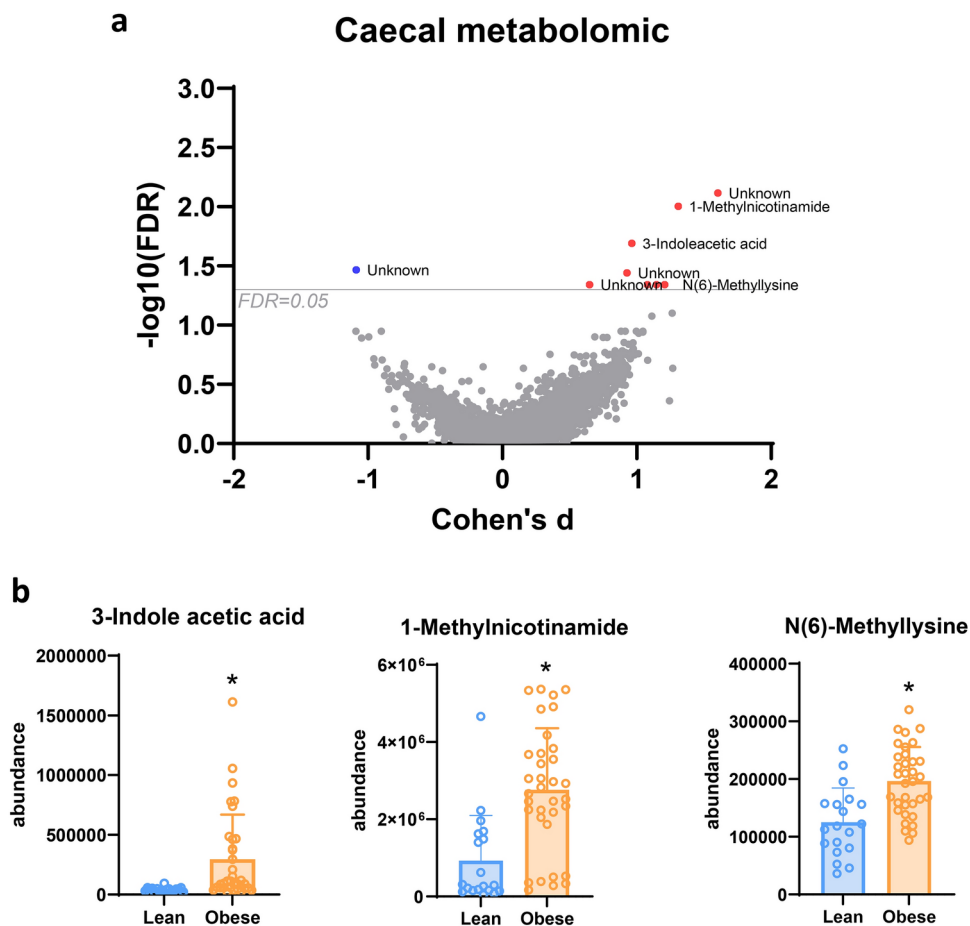


**Fig. 5.** Impact of obese microbiota transfer to mice on caecal metabolome. Volcano plot depicting the effect size (Cohen's  $d$ ) and  $-\log_{10}$  transformed  $q$  values derived from Welch's  $t$ -test analysis of the caecal metabolomic features different between obese recipient mice and lean recipient mice (a). The grey dots are features not significantly different, the red dots are features significantly up-regulated while the blue dots are features significantly down-regulated. Significantly altered ( $*q < 0.05$ , Welch's  $t$ -test) caecal identified metabolites (b). Data are means  $\pm$  SD.

components merits attention. Our data revealed that 3 amino acid-derived metabolites increased in the caecal content of obese-recipient mice compared to lean-recipient mice. The fold changes in abundance were 1.6, 3.0 and 7.1 for N(6)-methyllysine, 1-methylnicotinamide and I3A, respectively. Methyllysine was first described on a bacterial flagellar protein and thereafter was identified on eukaryotic histone proteins<sup>16</sup>. In fact, the lysine methylation of proteins has been established to regulate many cellular processes, including protein interactions and cellular signaling transduction. More importantly, I3A was also increased in the portal and systemic plasma even if the level of significance was not reached. The plasma and stool levels of I3A are directly regulated by the gut microbiota<sup>17</sup>. I3A is a tryptophan metabolite derived from gut microbiota. Tryptophan is one of the nine essential amino acids commonly found in protein-rich foods, such as milk, cheese, eggs, meat, fish, bananas, oats, nuts, and beans but also in normal chow diet for mice. Tryptophan is largely absorbed in the small intestine, and the fraction that reaches the colon is catabolized by numerous bacterial species, including *Escherichia coli*, *Clostridium*, *Bacteroides*, *Peptostreptococcus*, *Eubacterium*, and *Lactobacillus* species, and *Ruminococcus gnavus*<sup>18</sup>. Here, level of caecal I3A was particularly correlated to *Eubacteriaceae* and *Eubacterium*; the abundance of this family and genus being significantly increased in the caecal content of obese-recipient mice. Of note, the human origin of this microbe, particularly in the large intestine, is well documented<sup>19</sup>. Tryptophan-metabolizing pathways into I3A have already been identified in specific members of the human gut microbiota such as *Eubacterium hallii*<sup>20</sup>. This microbiota-derived indole metabolite has been identified as a postbiotic and a potent modulator of host physiology, maintaining in particular the homeostasis of the gut and systemic immunity<sup>21</sup>. It has been shown to ameliorate nonalcoholic fatty liver disease after sleeve gastrectomy and dextran-sulfate sodium-induced colitis in mice and has been proposed as potential treatment or prevention for dysbiosis-driven diseases<sup>17,22</sup>. There are several studies linking I3A to behavior<sup>23–25</sup>, but also that I3A supplementation can exert anti-depressive effects on an animal model of chronic stress<sup>26</sup>. However, while the present study highlights a negative correlation between circulating I3A and one of the behavioral parameters (anxiety via EPM test), no relationship between this metabolite and depression/anxiety mood in individuals with obesity has been documented in the literature. Inoculation of mice with microbiota from obese human donors stimulated dietary

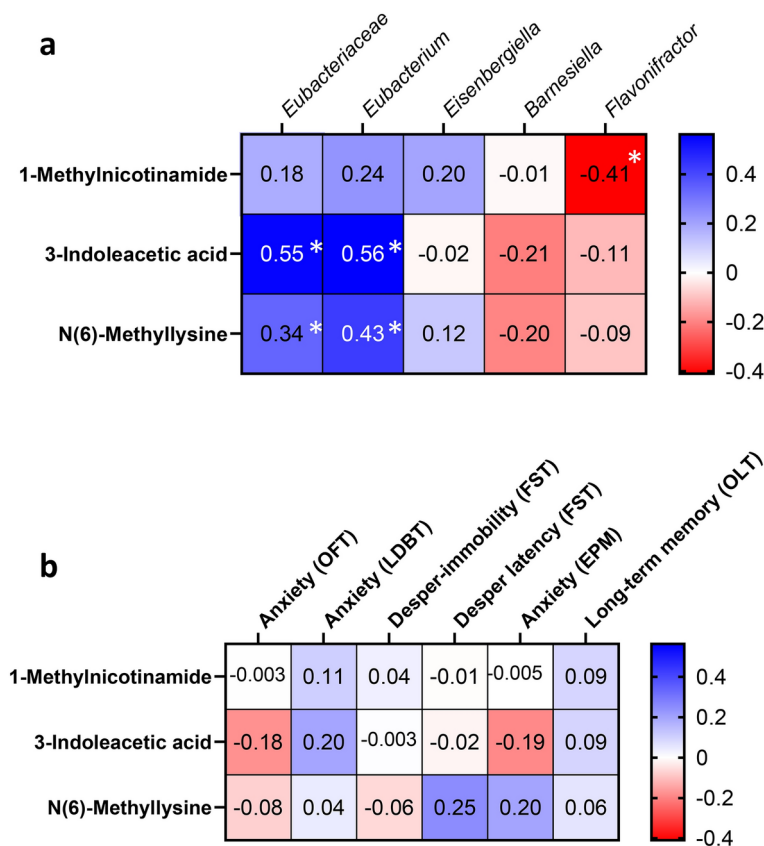


**Fig. 6.** Correlation analyses with caecal metabolites significantly altered with obese microbiota transfer. Heatmap of Spearman rank correlation between caecal metabolites and gut bacteria significantly altered by the obese microbiota transfer (a). Heatmap of Spearman rank correlation between caecal metabolites significantly altered by the obese microbiota transfer and the behavioral parameters (b). \* $p < 0.05$ .

tryptophan-dependent production of methylnicotinamide in the caecal content. Although no relationship was found with the abundance of a specific caecal bacteria, this vitamin B3 degradative product, was also shown to protect gut barrier function during experimental colitis<sup>27,28</sup>. In addition, this metabolite regulated insulin sensitivity in type 2 diabetic mice, leading to a reduction of hepatic glucose output and improvement of insulin resistance<sup>29</sup>. Early evidence of the association between methylnicotinamide and obesity was observed in metabolomic works since methylnicotinamide levels in human urine are positively correlated with the body mass index (BMI). Furthermore, methylnicotinamide levels in serum were found increased in the obese people and the methylnicotinamide levels in urine were found increased both in obese db/db mice and in obese Zucker rats<sup>30</sup>.

Altogether, our study suggests that inoculation of fecal microbiota from obese human donor to antibiotic-pretreated mice fed with chow diet leads to minor but persistent change in gut bacteria and intestinal microbial-derived metabolites without consequence on inflammation, metabolism and behavior.

## Methods

### Ethics statement

Mice experiments were performed in strict accordance with relevant guidelines and regulations for the care and use of animals and in accordance with the EU directive. All mouse experiments were approved by and performed in accordance with the guidelines of the local ethics committee for animal care of the Health Sector of the Université catholique de Louvain under the specific agreement numbers 2019/UCL/MD/009. Housing conditions were as specified by the Belgian Law of 29 May 2013, on the protection of laboratory animals. The study is reported in accordance with ARRIVE guidelines (<https://arriveguidelines.org>).

### Human donors

Ten donors with obesity were selected from the FOOD4GUT study that was a 3-month-long, multicentric, single-blind, placebo-controlled trial. The trial protocol was published on protocols.io (<https://doi.org/10.17504/protocols.io.baidica6>) and the trial was registered at ClinicalTrials.gov under identification number NCT03852069. Five control donors were obtained from the GUT2BRAIN cohort and were recruited in 2019. Recruitment, enrollment, randomization, sample size determination, inclusion and exclusion criteria, and outcomes have been previously described<sup>31,32</sup> for FOOD4GUT and GUT2BRAIN studies, respectively. Characteristics of the

donors are given in the Table S1. Both studies were approved by the “Comité d'éthique Hospitalo-facultaire Saint-Luc UCLouvain” (2014/26SEP/48 with amendment obtained on 18/03/2019 and 2014/14AOU/438 with amendment obtained on 22/10/2015, respectively) and in accordance to the written informed consent provided by participants (leaving the possibility to use biological material for future research outside the context of the FOOD4GUT study and GUT2BRAIN study). Both studies have been carried out in accordance with followed the ethical guidelines set out in the Declaration of Helsinki. All participants provided written informed consent in compliance with the European law 2001/20/CE guidelines, before inclusion.

### Experimental design

Specific pathogen-free (SPF) C57BL/6J male mice (Janvier Labs, Le Genest St Isle, France) were housed in a controlled environment (12 h daylight cycle) in individually ventilated cages with free access to food and water. Mice (aged 4–5 weeks) were inoculated with the fecal material from 10 patients with obesity (Obese-recipient mice) versus 5 control individuals (Control-recipient mice) (Fig. 1) according to previous procedures<sup>4,12</sup>. We have already demonstrated that, with such a protocol, the microbial composition of the recipient mice was similar to their human inoculum and was stable up to 6 weeks<sup>12</sup>. Mice were first administered broad-spectrum antibiotics cocktail (ampicillin, neomycin, metronidazole: 100 mg/kg; vancomycin: 50 mg/kg) by oral gavage once a day using flexible plastic feeding tubes (Instech Laboratories, the Netherlands) for 8 days. Amphotericin-B (1 mg/kg) was added to the antibiotic cocktail for the first 3 days to prevent fungi overgrowth. At the end of the antibiotic treatment, mice were subjected to intestinal purge with PEG 4000 (polyethylene glycol, macrogolum; 59 g/l supplemented with NaCl: 1.46 g/l; KCl: 0.75 g/l; Na<sub>2</sub>SO<sub>4</sub>: 5.68 g/l; NaHCO<sub>3</sub>: 1.68 g/l) in order to wash out the antibiotics remaining in the intestine. 1.5 ml of this intestinal bowel cleansing solution was administered by oral gavage to each mouse (2 × 500 µl the day before FMT with 1 h interval, and 1 × 500 µl 4h before the FMT). Mice were fasted 4 h before PEG administration. Handling of human fecal samples (previously collected in sterile containers and stored at – 80 °C) was performed under anaerobic conditions (vinyl anaerobic chamber, Coy Lab, MI, USA). Each fecal sample (0.5 g) was suspended in 5 ml of reduced sterile PBS (0.05% L-cysteine-HCL and N<sub>2</sub>), then vortexed for 5 min followed by sedimentation for 5 min. The slurry was then passed through a 100 µm cell strainer and 200 µl of the suspension was immediately administered to the mice by oral gavage with flexible disposable plastic tubes. Aliquots of this suspension were frozen at – 80 °C with 10% glycerol for the next gavages. Stool samples were inoculated 3 times in total (one time per day every 2 days) into recipient-mice (4 mice per donors). Before and after the inoculation with stool samples, all mice were fed a standard diet (AIN-93M en pellets, mature rodent diet, ResearchDiets) for up to 7 weeks.

### Behavioral testing

Behavioral testing started 20 days after the first FMT. All behavioral tests were recorded by a video camera connected to a computer and data analyse was performed by using EthoVision XT software (Noldus, the Netherlands), except for the forced swim test which was assessed manually. Three sessions of animal handling were performed 1 week before the first behavioral test to reduce the level of stress induced by the experimenter. Mice were transported to the behavioral testing room for a 1 h habituation period. All tests have been performed during the light phase. Each apparatus was thoroughly cleaned with water and dried between each animal. Control-recipient and Obese-recipient mice were tested in a random order and allowed to rest for several days between each test. The experimenter was not blinded to the group allocation when performing the testing.

#### *Elevated plus maze (EPM) test*

Mice were tested in the EPM apparatus which is elevated at 76 cm off the ground and consisting of 4 arms—2 open arms and 2 closed arms made with black Plexiglas walls<sup>33</sup>. The mouse was placed in the intersection of the 4 arms, facing an open arm, and allowed to explore for 5 min. Time spent and number of entries in the open arms were used to assess anxiety-like behavior.

#### *Open field (OF) test*

Animal was transferred to the open-field apparatus (40 cm × 40 cm) and was allowed to freely explore the new environment for 10 min. EthoVision XT software allowed the analyse of mobility pattern of each mouse, total distance traveled (cm) and time spent in the central area of the arena (percentage).

#### *Object location (OL) test*

Visual cues were placed in the room and kept constant during all tests. These tests consist of an acquisition phase (5 min) and a test phase (5 min), with an inter-test interval (ITI) of 24 h. The arena is open, made of plastic and measuring 40 cm × 40 cm with walls 16 cm high and a light intensity of 15 Lux. During the 5 min training, mice were placed in the arena and were allowed to freely explore two new and similar objects spaced 15 cm apart. We measured the time spent exploring each object. During the test phase, one of the objects from the training phase was moved. Both objects and arena were cleaned with 10% of ethanol between tested animals. We measured the time spent exploring each object for 5 min.

#### *Light-dark box (LDB) test*

Mice were placed for 10 min in a clear Plexiglas enclosure containing a black insert on one side. Time spent and number of entries in the light zone were used to assess anxiety-like behavior<sup>34</sup>.

#### *Forced swim (FS) test*

Mice were placed in an inescapable transparent Plexiglas tank (30 cm 320 cm) fill with autoclaved water (15 cm from the bottom) at room temperature<sup>35</sup>. A video camera recorded each mouse for 6 min and manual scoring

was performed by a trained experimenter who was blinded to the group allocation. Duration of immobility and latency to immobility were used to assess depression-like behavior. Water was renewed between each mouse. Before returning to their home cage, mice were gently dried with paper towels.

### Oral glucose tolerance test (OGTT)

One week before the end of the experiment, mice were fasted for 6 hours before being given an oral gavage glucose load (2 g glucose per kg body weight). Blood glucose was measured 30 minutes before (timepoint -30), just prior to the oral glucose load (timepoint 0) and then after 15, 30, 60, 90 and 120 min. Blood glucose was determined with a glucometer (Accu Chek Performa, Roche, Basel, Switzerland) on blood samples collected from the tip of the tail vein. Plasma insulin concentration was determined by ELISA (Mercodia, Uppsala, Sweden) according to the manufacturer's instructions.

### Blood and tissue sampling

Mice were anesthetized with isoflurane (Forene<sup>®</sup>, Abbott, England) and blood from portal vein and vena cava was centrifuged and serum/plasma samples were stored at -80 °C until analyses. Mice were then killed by decapitation. Brain, liver, subcutaneous adipose tissue and gut (ileum, colon, caecum) were weighted and immediately snap-frozen with liquid nitrogen then stored at -80 °C.

### Plasma parameters

Plasma samples obtained from vena cava were used to measure corticosterone (Enzo Life Sciences, Belgium) following manufacturer's instructions. Other markers -Tumor necrosis factor alpha, interleukin 1 beta, monocyte chemoattractant protein-1, C-X-C motif chemokine ligand 1, fibroblast growth factor 21, brain-derived neurotrophic factor, leptin- were determined using the Meso Scale Discovery (MSD) U-PLEX assay (Rockville, MD, USA) following the manufacturer's instructions.

### Gut microbiota analyses

The composition of the gut microbiota was analyzed by Illumina sequencing of the 16S rRNA gene, as previously described<sup>36</sup>. We followed the STORMS guidelines for human microbiome research<sup>37</sup>. DNA was extracted from faecal samples following the protocol Q described by Costea et al.<sup>38</sup> and uses the QIAamp DNA Stool Mini Kit (Qiagen, Germany) and includes a bead-beating step. Treatment with RNase A was performed (10 mg/ml, Thermo Fisher Scientific, USA). DNA concentration was determined, and purity (A260/A280) was checked using a NanoDrop 2000 (Thermo Fisher Scientific, USA). Absolute quantification of the total bacterial load was performed by quantitative polymerase chain reaction (qPCR) using the primers Bacteria Universal P338F (ACTCCTACGGGAGGCAGCAG) and P518r (ATTACCGCGGCTGCTGG). Real-time PCR was performed with a QuantStudio3 (Applied Biosystems, The Netherlands) using SYBR Green (GoTaq<sup>®</sup> qPCR mix, Promega, USA) for detection. All samples (0.1 ng/μl) were run in duplicate in a single 96-well reaction plate. Final concentrations were as follow: cDNA 2 μl/25 μl, primers 300 nM, and SyberGreen mix 1X (MeteorTaq DNA polymerase, dNTP, RT buffer, MgCl<sub>2</sub> 4 mM, SYBR<sup>®</sup> Green I, ROX passive reference and stabilizers, as provided by the manufacturer). Thermocycling conditions were as follow: initiation step at 95 °C 2 min; cycling stage at 95 °C 30 s, 60 °C 30 s, 72 °C 30 s, 40 cycles; melt curve stage at 95 °C 1 s, 65 °C 20 s, increment of 0.1 °C every 1 s until reaching 95 °C. Threshold was manually adjusted to reach the linear range of the log-fluorescent curves and CT values were determined using the QuantStudio Software (Version 1.4.3, Applied Biosystems, The Netherlands). Absolute quantification was achieved through the inclusion of a standard curve (performed in duplicate) on each plate generated by diluting DNA from pure culture of *L. acidophilus* NCFM (fivefold serial dilution). Cell counts were determined by plating and expressed as "colony-forming unit" (CFU) before DNA isolation. Amplicon sequencing of the microbiome was done at the University of Minnesota Genomics Centre. Briefly, the V5-V6 region of the 16S rRNA gene was PCR-enriched using the primer pair V5F\_Nextera (TCGTCGGCAGCGTCAGATGTGTATAAGAGACAGRGGATTAGATACCC) and V6R\_Nextera (GTCTCGTGGGCTCGGAGATGTGTATAAGAGACAGCACCRRCCATGCANCACT) in a 25 μl PCR reaction containing 5 μl of template DNA, 5 μl of 2× HotStar PCR master mix, 500 nM of final concentration of primers and 0.025 U/μl of HostStar Taq+ polymerase (QIAGEN). PCR-enrichment reactions were conducted as follows: an initial denaturation step at 95 °C for 5 min followed by 25 cycles of denaturation (20 s at 98 °C), annealing (15 s at 55 °C), and elongation (1 min at 72 °C), and a final elongation step (5 min at 72 °C). Next, the PCR-enriched samples were diluted 1:100 in water for input into library tailing PCR. The PCR reaction was analogous to the one conducted for enrichment except with a KAPA HiFi Hot Start Polymerase concentration of 0.25 U/μl, while the cycling conditions used were as follows: initial denaturation at 95 °C for 5 min followed by 10 cycles of denaturation (20 s at 98 °C), annealing (15 s at 55 °C), and elongation (1 min at 72 °C), and a final elongation step (5 min at 72 °C). The primers used for tailing are the following: F-indexing primer AATGATA CGGCGACCACCGAGATCTACAC[i5]TCGTCGGCAGCGTC and R-indexing primer CAAGCAGAAGACG GCATACGAGAT[i7]GTCTCGTGG GCTCGG, where [i5] and [i7] refer to the index sequence codes used by Illumina. The resulting 10 μl indexing PCR reactions were normalized using a SequalPrep normalization plate according to the manufacturer's instructions (Life Technologies). 20 μl of each normalized sample was pooled into a trough, and a SpeedVac was used to concentrate the sample pool down to 100 μl. The pool was then cleaned using 1X AMPureXP beads and eluted in 25 μl of nuclease-free water. The final pool was quantitated by QUBIT (Life Technologies) and checked on a Bioanalyzer High-Sensitivity DNA Chip (Agilent Technologies) to ensure correct amplicon size. The final pool was then normalized to 2 nM, denatured with NaOH, diluted to 8 pM in Illumina's HT1 buffer, spiked with 20% PhiX, and heat denatured at 96 °C for 2 min immediately prior to loading. A MiSeq 600 cycle v3 kit was used to sequence the pool. Subsequent bioinformatics analyses were performed in-house as previously described<sup>36</sup>. Initial quality filtering of the reads was performed with

the Illumina Software, yielding an average of 91468 pass-filter reads per sample. Quality scores were visualized with the FastQC software (<http://www.bioinformatics.babraham.ac.uk/publications.html>), and reads were trimmed to 220 bp (R1) and 200 bp (R2) with the FASTX-Toolkit ([http://hannonlab.cshl.edu/fastx\\_toolkit/](http://hannonlab.cshl.edu/fastx_toolkit/)). Next, reads were merged with the merge-illumina-pairs application v1.4.2 (with  $p = 0.03$ , enforced Q30 check, perfect matching to primers which are removed by the software, and otherwise default settings including no ambiguous nucleotides allowed). The UPARSE pipeline implemented in USEARCH v11 was used to further process the sequences. Amplicon sequencing variants (ASVs) were identified using UNOISE3. Such method infers the biological sequences in the sample prior to the introduction of amplification and sequencing errors and distinguishes sequence variants differing by as little as one nucleotide. The analysis allowed the identification of 4047 ASVs. ASVs were identified using the RDP database v16. Taxonomic prediction was performed using the `nbc_tax` function, an implementation of the RDP Naive Bayesian Classifier algorithm. Taxonomic identification of ASV of interest was refined using EZBioCloud (database version 2023.08.23) and cross-validated using `blastn` and the Prokaryota experimental taxonomic nt database. Alpha diversity indexes were calculated using QIIME on the rarefied ASV table. Rarefaction was performed using Mothur 1.32.1 by randomly selecting 43323 sequences for all samples. The dendrogram was generated through a hierarchical clustering (Ward D2 method) of the Aitchinson distance between samples (namely the euclidian distance between CLR-transformed relative abundance levels).

## Nontargeted metabolomics analyses

### *Sample preparation*

Three sample types were used for the non-targeted metabolomics analysis in this study—vena cava serum, portal serum and caecal content. Serum samples were prepared and analyzed separately from caecal content. All samples were randomized prior to pre-treatment and prepared as described in Klåvus et al.<sup>39</sup>. In brief, serum samples were allowed to thaw on wet ice and once thawed, 100  $\mu$ l of sample was mixed with 400  $\mu$ l of ice-cold LC-MS grade acetonitrile (Riedel de Haën, Honeywell, Seelze, Germany) in a separate tube. Precipitation was facilitated by 2-minute vortexing in room temperature followed by centrifugation for 5 min at 7000 $\times$ g at 4 °C. Supernatant was filtered using a PTFE 0.2  $\mu$ m syringe filter into a new tube and aliquoted into a brown LC-MS vial holding an insert. A separate QC vial was prepared by combining 10  $\mu$ l of filtered supernatant from all samples into a single vial. Ready samples were kept at – 20 °C until analysis. Solvent blanks consisted of solvent without additional treatments while extraction blanks devoid of sample followed the same treatment steps as samples.

Pre-weighted caecal samples were allowed to thaw on wet ice and mixed with 80% LC-MS grade MeOH (Riedel de Haën, Honeywell, Seelze, Germany) in a ratio of 500  $\mu$ l solvent per 100 mg of sample. Precipitation was facilitated by 5-minute vortexing in room temperature followed by centrifugation for 20 min at 17,000 $\times$ g at 4 °C. Filtration, QC and blanks preparations were the same as with the serum samples. Ready caecal extracts were kept at – 20 °C until analysis.

### *LC-MS measurement*

Bruker Impact II QTOF-MS instrument couple to an Elute UHPLC 1300 LC system (Bruker Daltonic, Bremen, Germany) was utilized for all non-targeted metabolomics data acquisition. Prior data acquisition the MS was calibrated using a sodium formate solution. Sample tray was at 4 °C and injection volume at 2  $\mu$ l for all samples. Serum samples were run in a separately from caecum samples. For both sample types, the sequence consisted of blank, extraction blank and QC injections prior to sample analysis with QC injections repeated every 13th injection. MS/MS data was acquired from QC sample and a randomly selected sample for each sample type using separately collision energies of 10, 20 and 40 eV. Data was acquired with both ESI+ and ESI– ionization. For the chromatographic separation a reversed-phase and HILIC chromatographies were employed resulting in a total of four datasets. The column applied in reversed-phase chromatography was Zorbax Eclipse XDB-C18, 1.8  $\mu$ m, 2.1  $\times$  100 mm (Agilent Technologies, Santa Clara, CA, USA) and the gradient at 0.4 ml/min flow rate consisted of 0–10 min: 2  $\rightarrow$  100% B, 10–14.5 min 100% B, 14.5–14.51 min 100  $\rightarrow$  2% B, 14.51–16.5 min 2% B where A: H<sub>2</sub>O + 0.1 % formic acid and B: MeOH + 0.1% formic acid (VWR HiPerSolv CHROMANORM, Radnor, PA, USA). The column applied in HILIC chromatography was Acquity UPLC® BEH Amide 1.7  $\mu$ m, 2.1  $\times$  100 mm (Waters Corporation, Milford, MA, USA) and gradient at 0.6 ml/min flow rate consisted of 0–2.5 min: 100% B, 2.5–10 min: 100% B  $\rightarrow$  0% B, 10–10.01 min: 0% B  $\rightarrow$  100% B, 10.01–12.5 min: 100% B where A: ACN:H<sub>2</sub>O (1:1) and B (ACN:H<sub>2</sub>O (9:1)) both containing 20 mM of ammonium formate (Arcos Organics, Geel, Belgium).

MS instrument source parameters were selected as indicated; a capillary voltage of 3500C, end plate offset voltage of 500V, temperature of 325 °C, dry gas flow of 10 L/min and nebulizer pressure of 45 psi. Parameters for the full scan mode were mass range of 50–1600 m/z, abundance threshold of 150 and scan time of 1.67 Hz. Parameters for the MS/MS scans were mass range of 50–1600 m/z, scan time of 1.67 Hz, number of precursors set to 4, active exclusion enabled with exclusion after 2 spectra and release after 0.25 min. Data was stored in centroid mode and instrument operated with the Bruker Compass HyStar SR 5.0 software

### *Peak picking, alignment and data pre-processing*

Before proceeding to peak picking, raw instrumental file (.d) were transformed into .mzML-format using the Bruker DataAnalysis 5.1 software. mzML-files were imported into MS-DIAL v 4.80 software used for peak picking and alignment<sup>40</sup>. Parameters for the peak picking included MS1 tolerance 0.005 Da, MS2 tolerance 0.015 Da, m/z range 0–2000 Da, minimum peak height 8000 (serum) or 10,000 (caecum), minimum peak width 8 scans, retention time tolerance 0.1 minutes, N% detected in at least one group 10 (serum) or 25 (caecum) and gap filling by compulsion activated. Peak picking and alignment was separately for each of the four datasets, results exported as .xlsx table and finally merged into a single .xlsx table.

The resulting .xlsx table was processed with *notame* v. 0.2.1 R package using R v. 4.0.3 (CRAN hosted by the Institute for Statistics and Mathematics of Wirtschafts Universität Wien, Austria). Each mode was pre-processed individually including drift correction, feature quality assessment and relevant visualizations. Shortly, first zero values were replaced with NA and features with QC detection below 30 % were flagged. Next, log-transformation was applied following drift correction by regularized cubic spline regression based on the QC samples. To prevent overfitting, smoothing parameter ranging from 0.5 to 1.5 was applied by leave-one-out cross-validation. After drift correction, log-transformed features were reverted to original scale to assess quality by flagging additional poor features if for example presence was less than 20 % in any group or having an RSD value of over 20 %. Random forest imputation was applied to impute missing values first on the good-quality (unflagged) features and then on all features.

#### Metabolite identification

Features were annotated using MS-DIAL v.4.80 and Bruker DataAnalysis 5.1 softwares to compare *m/z* and retention time values and MS/MS fragmentation spectra against in-house and publicly available databases such as LIPIDMAPS (<https://lipidmaps.org/>) and METLIN<sup>41</sup>. Features were selected for annotation based on their group-wise significance in multivariate and univariate analysis in addition to presence of MS/MS spectrum. Level of identification was assessed according to the recommendations listed by Chemical Analysis Working Group (CAWG) Metabolomics Standards Initiative (MSI)<sup>42</sup>: 1 = identified based on a reference standard, 2 = putatively annotated based on physicochemical properties or similarity with public spectral libraries, 3 = putatively annotated to a chemical class and 4 = unknown (2). Additionally, the remaining unknowns with MS/MS spectrum were subjected for analysis by MS-FINDER v 3.50<sup>43</sup> to characterize their molecular formula.

#### Statistical analysis

Data are expressed as means  $\pm$  SD or medians with interquartile ranges. Unpaired t tests or Mann-Whitney tests were used to compare Obese-recipient versus Control-recipient mice considering the normality of the distribution. For metabolomic analyse, multivariate analyses, namely PCA for dimension reduction and sPLS-DA for group discrimination, were conducted by 'mixOmics' R package v. 6.14.1 (58). For the sPLS-DA model, we used a cross-validation (CV) procedure of 10-fold CV repeated 50 times. Univariate analyses were conducted by 'notame' R package v. 0.2.1<sup>39</sup>. Significant features were shortlisted using Welch's t-test and VIP value  $>$  1.5 retrieved from the sPLS-DA model. All p-values were corrected using the Benjamini–Hochberg false discovery rate (FDR) to calculate the q-value. Correlation between the variation of bacteria (at the family level or the genus level) and metabolites significantly affected (Obese- versus Control-recipient mice) was assessed by Spearman's correlation tests. Statistical p values  $<$  0.05 were considered significant except for metabolomic and microbial abundances analyses for which only q values  $<$  0.05 were considered statistically significant. All analyses and graphs were conducted with Graphpad Prism software v. 10.1.2 (San Diego, CA, USA; [www.graphpad.com](http://www.graphpad.com)) except for the gut microbiota analyse and metabolomic analyse where we used R version 4.2.1 (CRAN hosted by the Institute for Statistics and Mathematics of Wirtschafts Universität Wien, Austria).

#### Data availability

Raw 16S rRNA gene sequences can be found in the SRA database (project ID: PRJNA1217873) and will be made public upon acceptance (person to contact Audrey Neyrinck: [audrey.neyrinck@uclouvain.be](mailto:audrey.neyrinck@uclouvain.be)). All data will be available from the corresponding author on reasonable request.

Received: 30 September 2024; Accepted: 16 April 2025

Published online: 02 May 2025

#### References

- Kootte, R. S. et al. Improvement of insulin sensitivity after lean donor feces in metabolic syndrome is driven by baseline intestinal microbiota composition. *Cell Metab.* **26**, 611–619. <https://doi.org/10.1016/j.cmet.2017.09.008> (2017).
- de Groot, P. F., Frissen, M. N., de Clercq, N. C. & Nieuwdorp, M. Fecal microbiota transplantation in metabolic syndrome: History, present and future. *Gut Microbes* **8**, 253–267. <https://doi.org/10.1080/19490976.2017.1293224> (2017).
- Turnbaugh, P. J. et al. The effect of diet on the human gut microbiome: A metagenomic analysis in humanized gnotobiotic mice. *Sci. Transl. Med.* **1**, 6–14. <https://doi.org/10.1126/scitranslmed.3000322> (2009).
- Rodriguez, J. et al. Discovery of the gut microbial signature driving the efficacy of prebiotic intervention in obese patients. *Gut* **69**, 1975–1987. <https://doi.org/10.1136/gutjnl-2019-319726> (2020).
- Clark, T. D., Reichelt, A. C., Ghosh-Swaby, O., Simpson, S. J. & Crean, A. J. Nutrition, anxiety and hormones. Why sex differences matter in the link between obesity and behavior. *Physiol. Behav.* **247**, 113713. <https://doi.org/10.1016/j.physbeh.2022.113713> (2022).
- Donoso, F., Cryan, J. F., Olavarria-Ramirez, L., Nolan, Y. M. & Clarke, G. Inflammation, lifestyle factors, and the microbiome-gut-brain axis: Relevance to depression and antidepressant action. *Clin. Pharmacol. Ther.* **113**, 246–259. <https://doi.org/10.1002/cpt.2581> (2023).
- Cryan, J. F. et al. The microbiota-gut-brain axis. *Physiol. Rev.* **99**, 1877–2013. <https://doi.org/10.1152/physrev.00018.2018> (2019).
- Ahmed, H. et al. Microbiota-derived metabolites as drivers of gut-brain communication. *Gut Microbes* **14**, 2102878. <https://doi.org/10.1080/19490976.2022.2102878> (2022).
- Idle, J. R. & Gonzalez, F. J. Metabolomics. *Cell Metab.* **6**, 348–351. <https://doi.org/10.1016/j.cmet.2007.10.005> (2007).
- Puljiz, Z. et al. Obesity, gut microbiota, and metabolome: From pathophysiology to nutritional interventions. *Nutrients* **15**, 236. <https://doi.org/10.3390/nu15102236> (2023).
- Leyrolle, Q. et al. Microbiota and metabolite profiling as markers of mood disorders: A cross-sectional study in obese patients. *Nutrients* **14**, 147. <https://doi.org/10.3390/nu14010147> (2021).
- Leclercq, S. et al. Gut microbiota-induced changes in  $\beta$ -hydroxybutyrate metabolism are linked to altered sociability and depression in alcohol use disorder. *Cell Rep.* **33**, 108238. <https://doi.org/10.1016/j.celrep.2020.108238> (2020).

13. Turnbaugh, P. J., Bäckhed, F., Fulton, L. & Gordon, J. I. Diet-induced obesity is linked to marked but reversible alterations in the mouse distal gut microbiome. *Cell Host Microbe* **3**, 213–223. <https://doi.org/10.1016/j.chom.2008.02.015> (2008).
14. Turnbaugh, P. J. et al. An obesity-associated gut microbiome with increased capacity for energy harvest. *Nature* **444**, 1027–1031. <https://doi.org/10.1038/nature05414> (2006).
15. Rodríguez, D. M., Benninghoff, A. D., Aardema, N. D. J., Phatak, S. & Hintze, K. J. Basal diet determined long-term composition of the gut microbiome and mouse phenotype to a greater extent than fecal microbiome transfer from lean or obese human donors. *Nutrients* **11**, 630. <https://doi.org/10.3390/nu11071630> (2019).
16. Bhat, K. P., Ümit Kaniskan, H., Jin, J. & Gozani, O. Epigenetics and beyond: Targeting writers of protein lysine methylation to treat disease. *Nat. Rev. Drug Discov.* **20**, 265–286. <https://doi.org/10.1038/s41573-020-00108-x> (2021).
17. Wang, Y. et al. Role of indole-3-acetic acid in NAFLD amelioration after sleeve gastrectomy. *Obes. Surg.* **31**, 3040–3052. <https://doi.org/10.1007/s11695-021-05321-0> (2021).
18. Liu, M., Nieuwdorp, M., de Vos, W. M. & Rampanelli, E. Microbial tryptophan metabolism tunes host immunity, metabolism, and extraintestinal disorders. *Metabolites* **12**, 834. <https://doi.org/10.3390/metabo12090834> (2022).
19. Wishart, D. S. et al. MiMeDB: The human microbial metabolome database. *Nucleic Acids Res.* **51**, D611–D620. <https://doi.org/10.1093/nar/gkac868> (2023).
20. Russell, W. R. et al. Major phenylpropanoid-derived metabolites in the human gut can arise from microbial fermentation of protein. *Mol. Nutr. Food Res.* **57**, 523–535. <https://doi.org/10.1002/mnfr.201200594> (2013).
21. Su, X., Gao, Y. & Yang, R. Gut microbiota-derived tryptophan metabolites maintain gut and systemic homeostasis. *Cells* **11**, 96. <https://doi.org/10.3390/cells11152296> (2022).
22. Qu, X. et al. Indole-3-acetic acid ameliorates dextran sulfate sodium-induced colitis via the ERK signaling pathway. *Arch. Pharm. Res.* **47**, 288–299. <https://doi.org/10.1007/s12272-024-01488-z> (2024).
23. Karu, N. et al. Tryptophan metabolism, its relation to inflammation and stress markers and association with psychological and cognitive functioning: Tasmanian Chronic Kidney Disease pilot study. *BMC Nephrol.* **17**, 171. <https://doi.org/10.1186/s12882-016-0387-3> (2016).
24. Anderson, G. M., Gerner, R. H., Cohen, D. J. & Fairbanks, L. Central tryptamine turnover in depression, schizophrenia, and anorexia: Measurement of indoleacetic acid in cerebrospinal fluid. *Biol. Psychiatry* **19**, 1427–1435 (1984).
25. Zheng, S. et al. Urinary metabonomic study on biochemical changes in chronic unpredictable mild stress model of depression. *Clin. Chim. Acta* **411**, 204–209. <https://doi.org/10.1016/j.cca.2009.11.003> (2010).
26. Chen, Y. et al. Indole acetic acid exerts anti-depressive effects on an animal model of chronic mild stress. *Nutrients* **14**, 19. <https://doi.org/10.3390/nu14235019> (2022).
27. Suntornsaratoun, P. et al. *Lactobacillus rhamnosus* GG stimulates dietary tryptophan-dependent production of barrier-protecting methylnicotinamide. *Cell Mol. Gastroenterol. Hepatol.* **18**, 101346. <https://doi.org/10.1016/j.jcmgh.2024.04.003> (2024).
28. Nejabati, H. R. et al. N1-methylnicotinamide: Is it time to consider it as a dietary supplement for athletes? *Curr. Pharm. Des.* **28**, 800–805. <https://doi.org/10.2174/138161282866220211151204> (2022).
29. Zhang, J., Chen, Y., Liu, C., Li, L. & Li, P. N(1)-methylnicotinamide improves hepatic insulin sensitivity via activation of SIRT1 and inhibition of FOXO1 acetylation. *J. Diabetes Res.* **2020**, 1080152. <https://doi.org/10.1155/2020/1080152> (2020).
30. Liu, J. R. et al. Roles of nicotinamide N-methyltransferase in obesity and type 2 diabetes. *Biomed. Res. Int.* **2021**, 9924314. <https://doi.org/10.1155/2021/9924314> (2021).
31. Hiel, S. et al. Link between gut microbiota and health outcomes in inulin-treated obese patients: Lessons from the Food4Gut multicenter randomized placebo-controlled trial. *Clin. Nutr.* <https://doi.org/10.1016/j.clnu.2020.04.005> (2020).
32. Leclercq, S. et al. Blood metabolomic profiling reveals new targets in the management of psychological symptoms associated with severe alcohol use disorder. *Elife* **13**, 937. <https://doi.org/10.7554/eLife.96937> (2024).
33. Sidor, M. M., Rilett, K. & Foster, J. A. Validation of an automated system for measuring anxiety-related behaviours in the elevated plus maze. *J. Neurosci. Methods* **188**, 7–13. <https://doi.org/10.1016/j.jneumeth.2010.01.021> (2010).
34. Bourin, M. & Hascoët, M. The mouse light/dark box test. *Eur. J. Pharmacol.* **463**, 55–65. [https://doi.org/10.1016/S0014-2999\(03\)01274-3](https://doi.org/10.1016/S0014-2999(03)01274-3) (2003).
35. Can, A. et al. The mouse forced swim test. *J. Vis. Exp.* **1**, e3638. <https://doi.org/10.3791/3638> (2012).
36. Thibaut, M. M. et al. The microbiota-derived bile acid taurodeoxycholic acid improves hepatic cholesterol levels in mice with cancer cachexia. *Gut Microbes* **17**, 2449586. <https://doi.org/10.1080/19490976.2025.2449586> (2025).
37. Mirzayati, C. et al. Reporting guidelines for human microbiome research: the STORMS checklist. *Nat. Med.* **27**, 1885–1892. <https://doi.org/10.1038/s41591-021-01552-x> (2021).
38. Costea, P. I. et al. Towards standards for human fecal sample processing in metagenomic studies. *Nat. Biotechnol.* **35**, 1069–1076. <https://doi.org/10.1038/nbt.3960> (2017).
39. Klävus, A. et al. “notame”: Workflow for non-targeted LC-MS metabolic profiling. *Metabolites* **10**, 135. <https://doi.org/10.3390/metabo10040135> (2020).
40. Tsugawa, H. et al. MS-DIAL: Data-independent MS/MS deconvolution for comprehensive metabolome analysis. *Nat. Methods* **12**, 523–526. <https://doi.org/10.1038/nmeth.3393> (2015).
41. Smith, C. A. et al. METLIN: A metabolite mass spectral database. *Ther. Drug Monit.* **27**, 747–751. <https://doi.org/10.1097/01.ftd.000179845.53213.39> (2005).
42. Sumner, L. W. et al. Proposed minimum reporting standards for chemical analysis Chemical Analysis Working Group (CAWG) metabolomics standards initiative (MSI). *Metabolomics* **3**, 211–221. <https://doi.org/10.1007/s11306-007-0082-2> (2007).
43. Tsugawa, H. et al. Hydrogen rearrangement rules: Computational MS/MS fragmentation and structure elucidation using MS-FINDER software. *Anal. Chem.* **88**, 7946–7958. <https://doi.org/10.1021/acs.analchem.6b00770> (2016).

## Acknowledgements

We thank prof. Thissen and prof. de Timary to give access to stool sample collection from FOOD4GUT study and GUT2BRAIN study, respectively. We thank A. Flandin and B. Es Saadi for their excellent technical assistance. NMD is a recipient of grants from the Fonds de la Recherche Scientifique (FRS)-FNRS (Grant Numbers: PINT-MULTI R.8013.19 (NEURON, call 2019) and PDR T.0068.19). LBB is a Collen-Francqui Research Professor and grateful for the support of the Francqui Foundation. PDC is honorary research director at FRS-FNRS (Fonds de la Recherche Scientifique) and the recipient of grants from FNRS (Projet de Recherche PDR-convention: FNRS T.0030.21, FRFS-WELBIO: WELBIO-CR-2022A-02P, EOS: program no. 40007505) KH is a recipient of grants from the Research Council of Finland (grant numbers 321716 and 334814), and Jane and Aatos Erkkö Foundation.

## Author contributions

N.M.D., A.M.N. and Q.L. conceived the experiment(s). Q.L. conducted the experiment(s). H.A., T.M., O.K. and K.H. performed the analyse of the metabolomics data. A.M.N., H.A., Q.L., C.A. and L.B.B performed data ana-

lyse. A.M.N. and N.M.D. wrote the paper. S.Le, S.La., P.D.C., O.K., L.B.B. and K.H. provided intellectual input on the paper and reviewed the paper. N.M.D. planned and supervised all experiments and manuscript preparation. All authors reviewed the manuscript.

## Declarations

### Competing interests

OK and KH are founders of Afekta Technologies Ltd. PDC is inventor on patent applications dealing with the use of gut bacteria and their components in the treatment of diseases. PDC was co-founder of The Akkermansia Company and Enterosys. The other authors report no financial interests or potential conflicts of interest.

### Additional information

**Supplementary Information** The online version contains supplementary material available at <https://doi.org/10.1038/s41598-025-99047-z>.

**Correspondence** and requests for materials should be addressed to N.M.D.

**Reprints and permissions information** is available at [www.nature.com/reprints](http://www.nature.com/reprints).

**Publisher's note** Springer Nature remains neutral with regard to jurisdictional claims in published maps and institutional affiliations.

**Open Access** This article is licensed under a Creative Commons Attribution-NonCommercial-NoDerivatives 4.0 International License, which permits any non-commercial use, sharing, distribution and reproduction in any medium or format, as long as you give appropriate credit to the original author(s) and the source, provide a link to the Creative Commons licence, and indicate if you modified the licensed material. You do not have permission under this licence to share adapted material derived from this article or parts of it. The images or other third party material in this article are included in the article's Creative Commons licence, unless indicated otherwise in a credit line to the material. If material is not included in the article's Creative Commons licence and your intended use is not permitted by statutory regulation or exceeds the permitted use, you will need to obtain permission directly from the copyright holder. To view a copy of this licence, visit <http://creativecommons.org/licenses/by-nc-nd/4.0/>.

© The Author(s) 2025